

Oxovanadium(V) Tetrathiacalix[4]arene Complexes and Their Activity as Oxidation Catalysts

Elke Hoppe and Christian Limberg*^[a]

Abstract: With the aim of modeling reactive moieties and relevant intermediates on the surfaces of vanadium oxide based catalysts during oxygenation/dehydrogenation of organic substrates, mono- and dinuclear vanadium oxo complexes of doubly deprotonated *p*-tert-butylated tetrathiacalix[4]arene (H_2TC) have been synthesized and characterized: $PPh_4[(H_2TC)VOCl_2]$ (**1**) and $(PPh_4)_2\{[(H_2TC)V(O)(\mu-O)]_2\}$ (**2**). According to the NMR spectra of the dissolved complexes they both retain the structures adopted in the crystalline state, as revealed by single-crystal X-ray crystallography. Compounds **1** and **2** were tested as catalysts for the oxidation of alcohols with O_2 at 80 °C. Both **1** and **2** efficiently catalyze the oxida-

tion of benzyl alcohol, crotyl alcohol, 1-phenyl-1-propanol, and fluorenol, and in most cases dinuclear complex **2** is more active than mononuclear complex **1**. Moreover, the two thiacalixarene complexes **1** and **2** are in many instances more active than oxovanadium(V) complexes containing “classical” calixarene ligands tested previously. Complexes **1** and **2** also show significant activity in the oxidation of dihydroanthracene. Further investigations led to the conclusion that **1** acts as precatalyst that is converted to the

active species $PPh_4[(TC)V=O]$ (**3**) at 80 °C by double intramolecular HCl elimination. For complex **2**, the results of mechanistic investigations indicated that the oxidation chemistry takes place at the bridging oxo ligands and that the two vanadium centers cooperate during the process. The intermediate $(PPh_4)_2\{[H_2TCV(O)]_2(\mu-OH)(\mu-OC_{13}H_9)\}$ (**4**) was isolated and characterized, also with respect to its reactivity, and the results afforded a mechanistic proposal for a reasonable catalytic cycle. The implications which these findings gathered in solution may have for oxidation mechanisms on the surfaces of V-based heterogeneous catalysts are discussed.

Keywords: calixarenes • heterogeneous catalysis • oxidation • O ligands • vanadium

Introduction

Many economically important industrial processes are performed with heterogeneous catalysts. The active sites on such catalysts are often not well-defined, but it has been demonstrated that good activity and selectivity often stems from active sites consisting only of one or a few isolated metal centers.^[1,2] However, even with this confinement often many mechanistic possibilities remain open that must be understood if further optimization is to be achieved. A representative example is the oxidative dehydrogenation (ODH)

of light alkanes. Supported vanadium oxides are among the best catalysts for ODH of propane and also of methanol (\rightarrow formaldehyde),^[3] and a considerable amount of research has been devoted to the mechanisms of ODH reactions on supported vanadium-based catalysts.^[3h,i,j,4] To understand them, it is crucial to know where the individual reaction steps occur; for instance, at singly coordinated terminal oxo ligands or at bridging oxo sites (classification of the literature according to the suggested active oxo species is reviewed in reference [4i]). However, the acquisition of such knowledge is difficult with the common methods for the characterization of heterogeneous catalysts. Furthermore, even if the active sites are known, the clarification of questions concerning their reactivity is far more difficult than for homogeneous catalysts. However, working hypotheses for heterogeneous processes can provide an inspiration for the synthesis of molecular models^[5-7] that can be investigated in the homogeneous phase and thus, on the one hand, may serve to support or refute mechanistic proposals. On the other hand, such models can prove themselves as new homogeneous cat-

[a] E. Hoppe, Prof. Dr. C. Limberg
Humboldt-Universität zu Berlin
Institut für Chemie
Brook-Taylor-Strasse 2, 12489 Berlin (Germany)
E-mail: christian.limberg@chemie.hu-berlin.de

Supporting information for this article is available on the WWW under <http://www.chemeurj.org/> or from the author.

alysts, independent of the heterogeneous processes that prompted their synthesis.

The construction of molecular models for metal oxo surface sites requires ligands that are capable of mimicking the oxidic environments surrounding metal oxo moieties on oxidic supports or bulk materials, and in this context especially two ligand systems have established themselves: deprotonated silsesquioxanes^[6] and calixarenes.^[7] With regard to vanadium oxide catalyzed ODH, we have recently reported the synthesis of a variety of mono- and dinuclear calixarene-based vanadium(V) oxo complexes **I–IV**,^[8,9] which (along with some compounds published simultaneously^[13a]) complemented the few structurally characterized representatives existing till then.^[13b,c]

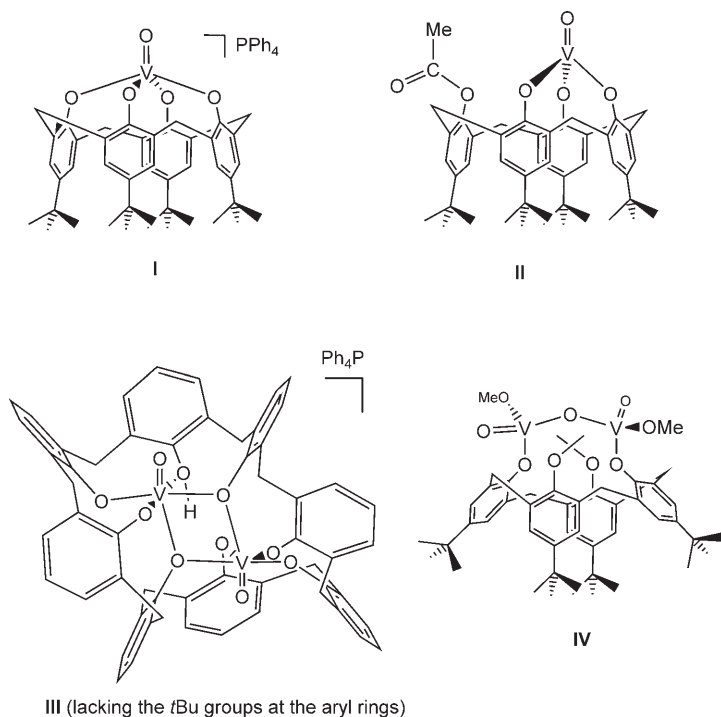
indeed efficient catalysts for the oxidation of activated alcohols with O₂.^[9] Furthermore, the dinuclear complexes are significantly more active than the mononuclear compounds: for instance, while singly charged mononuclear complex **I** is inert under various conditions, also towards other substrates, the two dinuclear complexes were capable of oxidizing an unfunctionalized hydrocarbon like 9,10-dihydroanthracene, although the TOFs are much lower than those determined for oxidation of alcohols. These findings may suggest increased activity through cooperative behavior of two metal centers, which may be applicable to heterogeneous ODH of methanol with vanadia catalysts. However, clearly a larger number of complexes must be synthesized and investigated—also with respect to the effective mechanisms—to support this hypothesis, and we therefore also considered thiacalixarenes as ligands.

Compared to the related *p*-*tert*-butylcalix[4]arene, the chemistry of thiacalixarenes is far less explored, which is not surprising considering that synthetic routes to thiacalixarenes and their sulfinyl and sulfonyl derivatives were developed only in the late 1990s.^[10] Investigations of their coordination chemistry showed that the thioether units do not behave innocently but take part in metal-ion coordination,^[11] so that the interaction of a transition metal ion with thiacalixarene-based ligands is usually stronger than with “classical” calixarenes, and this may lead to significant (advantageous) chemical differences. Here we report on oxovanadium(V) thiacalix[4]arene complexes and their behavior as alcohol oxidation catalysts.

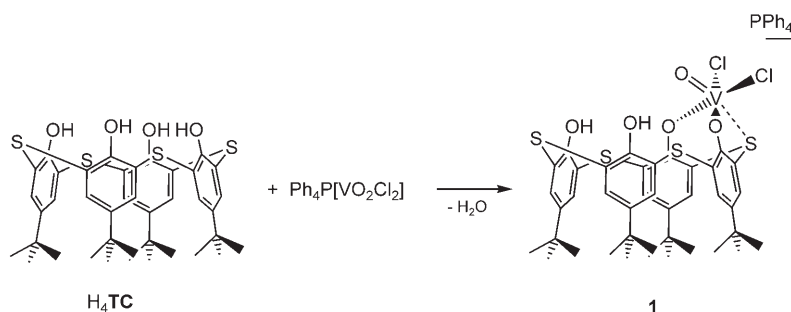
Results and Discussion

Complex synthesis: The *p*-*tert*-butyltetra-thiacalix[4]arene H₄TC can be readily prepared by known methods,^[10a,12] and it has been reported that NEt₃ is suitable as a base to deprotonate the phenolic functions.^[10a,12] In fact, the presence of NEt₃ (or lithium naphthalenide) was essential for the successful preparation of **I** from *p*-*tert*-butyl-calix[4]arene and Ph₄P[VO₂Cl₂].^[9] However, it turned out that H₄TC reacts with Ph₄P[VO₂Cl₂] in the absence of an external base, as indicated by a color change from light green to purple. After workup a purple crystalline material was obtained that was identified as PPh₄[(H₂TC)VO₂Cl₂] (**1**) (Scheme 1) by single-crystal X-ray crystallography, elemental analysis, and IR and NMR spectroscopy. The molecular structure of the anion of **1** is shown in Figure 1.

A noncrystallographic mirror plane passes through the center of the calixarene ligand and atoms V1, O1, and S3. The calixarene moiety has a cone conformation, and the vanadium center is positioned above the calix and is shifted by 0.3539(9) Å out of the plane defined by O2, O3, C11, and C12 in the direction of terminal ligand O1, whose bond length to the V center (1.592(4) Å) is typical for oxo ligands in oxovanadium(V) calixarene complexes.^[8,9,13] The coordination sphere of V is completed by one of the thioether groups of the ligand: the distance of 2.7553(16) Å to S3 is



To test these compounds as functional models for active sites during the ODH of alkanes and methanol their reactivities were investigated.^[9] Of course, such molecular models will be inert in contact with alkanes under the conditions applicable in molecular chemistry, as their conversion requires a C–H bond cleavage in the rate-determining step, which is characterized by a high barrier.^[4] This requires high temperatures—also in the case of the heterogeneous counterparts—that molecular models will not survive. However, alcohols are less inert as substrates, so that their oxidative dehydrogenation can also be investigated in the liquid phase, and any information derived from such studies may contribute to a more comprehensive understanding not only of methanol oxidation on vanadia catalysts, but may also even provide ideas about the (probably) more complex ODH of alkanes. We found that some of these model complexes are



Scheme 1.

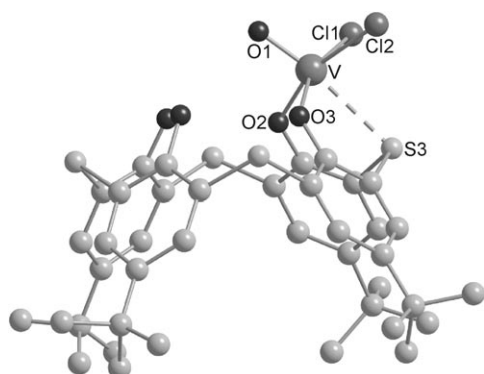


Figure 1. Molecular structure of the anion of **1**. All hydrogen atoms and the Ph_4P^+ cation omitted for clarity. Selected bond lengths [\AA] and angles [$^\circ$]: V–O1 1.592(4), V–O2 1.904(4), V–O3 1.877(5), V–Cl1 2.305(2), V–Cl2 2.308(2), V–S3 2.7553(16); O1–V–O2 97.18(18), O1–V–O3 98.81(18), O1–V–Cl1 101.28(15), O1–V–Cl2 102.06(15), O1–V–S3 172.50(15), V–(O2, O3, Cl1, Cl2) 0.3539(9).

shorter than the sum of the van der Waals radii of vanadium (1.34 \AA) and sulfur (1.85 \AA) and thus indicative of coordinative interaction. It is slightly longer than the corresponding distances in comparable compounds in which thioether functions are coordinated to vanadium (e.g., 2.689(1) \AA),^[14] which might be due to the strong *trans* influence of terminal oxo ligands (O1–V–S3 172.50(15) $^\circ$). Overall, the vanadium atom is located in a distorted octahedral coordination environment. The V–O2 and V–O3 bonds have almost the same lengths (1.904(4), 1.877(5) \AA), and the same is true of the V–Cl1 and V–Cl2 bonds (2.305(3), 2.308(2) \AA).

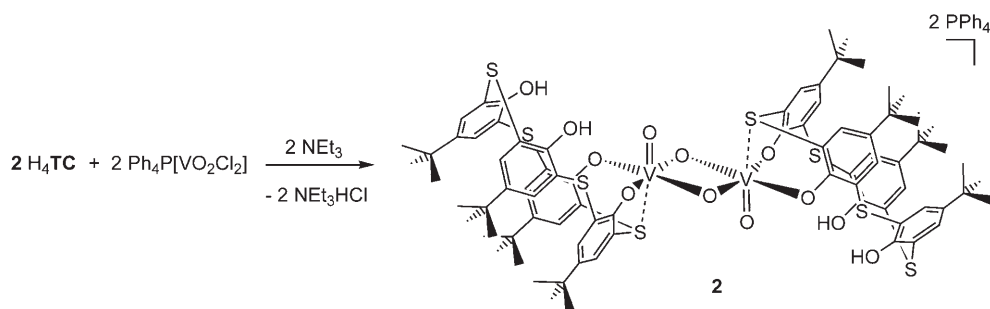
The structure of **1** in solution appears to be similar to that adopted in the crystal. The ^1H NMR spectroscopic data hint at the existence of an identical mirror plane: 1) Accordingly, only one signal (9.84 ppm) can be found for the two OH groups. 2) Additionally, such a C_s -symmetric structure should have two types of different aryl rings and the two protons belonging to each of these aryl rings should be magnetically different and couple to each other; therefore, altogether four doublets should be expected, and this is exactly what is found experimentally in the region where the aryl protons absorb. 3) Following the same arguments, two sin-

glets would be expected for the protons of the *tert*-butyl groups, and indeed these can be resolved in CD_2Cl_2 .

Compound **1** is also obtained when an excess of $\text{Ph}_4\text{P}[\text{VO}_2\text{Cl}_2]$ is employed in the reaction shown in Scheme 1, probably because a second $\text{Cl}_2(\text{O})\text{V}^+$ unit could not be bound to O5/O4 in the same way as the first one without prior rearrangements/reactions. The formation of **1** must have

proceeded via addition of two OH groups to one of the V=O groups of the starting material with elimination of water (similar reactivity was reported only recently for molybdenyl chemistry).^[15] Accordingly, in the absence of an external base the protons of H_4TC are acidic enough to attack one of the nucleophilic oxo atoms of $[\text{VO}_2\text{Cl}_2]^-$; as in the case of “normal” calixarenes, however, they are not acidic enough to further induce intramolecular HCl elimination: the anion of **1** formally still contains two equivalents of HCl whose elimination would lead to the thia analogue of **1**. The fact that such a complex is not formed spontaneously may to some extent be a result of the coordinative support at the vanadium center by the sulfur atom. On the other hand, formation of **1** requires addition of a base at least as strong as NEt_3 . Therefore, the reaction of Scheme 1 was repeated in the presence of NEt_3 , which led to the precipitation of a red solid. After purification and crystallization this was identified as $(\text{PPh}_4)_2[\{(\text{H}_2\text{TCV}(\text{O})(\mu\text{-O}))_2\}]$ (**2**) with the aid of an X-ray crystal structure determination, elemental analysis, and IR and NMR spectroscopy (Scheme 2). The molecular structure of the dianion of **2** is shown in Figure 2.

In the anion of **2** two O=V groups are linked by two bridging oxo ligands in a way that positions the terminal O ligands in an *anti* fashion, and—ignoring variations of the bond lengths and angles—approximately C_s symmetry with a mirror plane running through these oxovanadium(V) groups can be assigned to the complex anion. Each vanadium center is additionally coordinated by a calixarene ligand in a cone conformation through two phenolate groups; location of the vanadium center above the calix allows for additional interaction between V1 and S1. Accordingly, both vanadium atoms have distorted octahedral coordination geometries as in **1**, again with the terminal oxo ligands and the sulfur atoms in *trans* positions. The vanadium atom is situated 0.3548(7) \AA above the mean plane defined by O2, O3, O4, and O8, and the V=O1 bond length (1.6005(10) \AA) is comparable to that of **1**. However, the V–S1 interaction ($d(\text{V1}–\text{S1})=2.9446(11)$ \AA) is weaker than the corresponding one in **1** (2.7553(16) \AA), and accordingly the arrangement of the O1, V, and S1 atoms deviates more from a linear geometry (164.88(5) $^\circ$). The O–V single bonds differ significantly in length even when they are involved in the same type of bonding: naturally, bonds involving the bridging oxo ligands



Scheme 2.

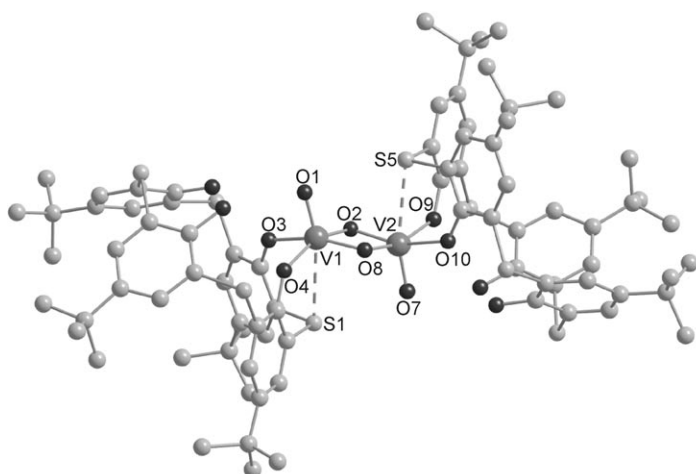


Figure 2. Molecular structure of the dianion of **2**. All hydrogen atoms, the Ph_4P^+ cations, and cocrystallized DMF solvent molecules omitted for clarity. Selected bond lengths [Å] and angles [°]: O1–V1 1.6005(10), O2–V1 1.8635(9), O3–V1 1.9985(10), O4–V1 1.900(1), O8–V1 1.8051(10), S1–V 2.9446(11); O1–V1–O2 105.38(7), O1–V1–O3 93.97(6), O1–V1–O4 99.38(4), O1–V1–O8 104.53(5), O1–V1–S1 164.88(5), V1–O2–V2 97.00(5), V1–O8–V2 97.79(6), V–(O2, O3, O4, O8) 0.3548(7), O7–V2 1.5987(10), O2–V2 1.8018(9), O8–V2 1.8383(11), O9–V2 1.9792(11), O10–V2 1.9993(10), S5–V2 2.8094(11), V2–(O2, O8, O9, O10) 0.3255(7), O7–V2–O2 106.11(5), O7–V2–O8 104.14(7), O7–V2–O9 94.16(5), O7–V2–O10 95.28(6), O7–V2–S5 164.86(5), V1–V2 2.7453(6).

are the shortest, but their lengths vary from 1.8018 to 1.8635 Å, so that the V_2O_2 core is quite asymmetric. As already observed to a smaller extent for **1**, the bond lengths of the phenolate oxygen atoms to the vanadium centers are somewhat longer than usually observed for V/phenolate units (ca. 1.8 Å), since this allows for more effective interaction with the S atom; again, broad variation is found, from 1.900(1) Å (O4–V) to 1.9993(10) Å (V–O10).

The ^1H NMR spectrum of **2** shows that on dissolution the overall symmetry is retained so that the same spectral features are observed for the aryl and *tert*-butyl protons as discussed for **1**.

The formation of **2** can be imagined to proceed by initial double HCl elimination assisted by NEt_3 , which apparently is now more favorable than attack at the terminal oxo ligands of $[\text{VO}_2\text{Cl}_2]^-$, followed by a dimerization of the resulting anions (formally $\text{H}_2\text{TCV}(\text{=O})\text{O}^-$) via two oxo ligands.

Thus, two novel oxovanadium thiacalixarene complexes were available, and it seemed interesting to investigate their potential as catalysts for ODH of alcohols with O_2 in comparison with the results obtained for **I–IV**.^[9]

Catalytic activity and evaluation of the potential as functional models for ODH:

Catalytic amounts of the complexes were dissolved in acetonitrile, and molecular sieves were added to remove the water produced during oxidation. After addition of a chosen alcohol, the resulting mixture was heated for 1–3 h to 80 °C under an oxygen atmosphere. After workup the ratios between the oxidized products (carbonyl compounds) were formed selectively, except for the case of dihydroanthracene) and unconsumed starting material were determined by NMR spectroscopy, and the turnover frequencies (TOFs) calculated. Since **II**, **IV**, and **2** have dinuclear cores whose V centers could in principle act independently and simultaneously, the amount of catalyst added was halved in these cases to allow comparison with mononuclear catalysts. Of course, if these catalysts use only one V center at a time, this procedure creates an artificially worse result for these compounds, but superiority of dinuclear versus mononuclear complexes can then safely be attributed to cooperative behavior of the vanadium centers. For evaluating TOFs, $\text{VO}(\text{acac})_2$ (acac = acetylacetonato) was chosen as reference system, as it was recently reported to efficiently catalyze the aerobic oxidation of 1-phenyl-1-propargyl alcohol.^[16] The results are summarized in Table 1 and Figure 3. First, three saturated, nonactivated alcohols were employed: 1-hexanol, 2-pentanol, and cyclohexanol. For none of them could any conversion be observed with complexes **I–IV**, **1**, and **2**. Among the classical calixarene oxovanadium complexes only **III** showed some activity in the oxidation of *both* of the primary alcohols benzyl alcohol and cinnamyl alcohol (1.7 and 3.5 h^{-1}), and $[\text{VO}(\text{acac})_2]$ performed notably better (12.3 and 50.0 h^{-1}), as it was also capable of oxidizing crotyl alcohol with a TOF of 9.0 h^{-1} .^[9] For all but one of the alcohols containing unsaturated (activating) units, **1** and **2** are significantly more active than **I–IV**, and **2** catalyzes the oxidation of benzyl alcohol (33.6 h^{-1}) and *trans*-crotyl alcohol (\rightarrow *trans*-2-butenal, 12.0 h^{-1}) even more efficiently than the reference system. The outstanding behavior of **2** is consistent with our previous observation^[9] that dinuclear complexes show better efficiency than corresponding mononu-

Table 1. Substrate oxidation with O₂ and 1 mol% **1** and 0.5 mol% **2** (as it contains two V centers) as catalysts in comparison with the results previously^[9] obtained with **I–IV** (1 mol% for mononuclear catalysts and 0.5 mol% for dinuclear catalysts) and [VO(acac)₂]. Data calculated on the basis of results after 3 h or 1 h (*) of reaction.

	TOF [h ⁻¹]					1	2
	I	II	III	IV	[VO(acac) ₂]		
cyclohexanol	0	0	0	0	0	0	0
1-hexanol	0	0	0	0	0	0	0
2-pentanol	0	0	0	0	0	0	0
benzyl alcohol	0	0	1.7	0	12.3	27.1*	33.6*
cinnamyl alcohol	0	1.7	3.5	10.2	50.0*	27.0*	45.0*
<i>trans</i> -crotyl alcohol	0	0	0	0	9.0	4.3	12.0
1-phenyl-1-propargylic alcohol	0.7	2.3	12.9	7.7	60.0*	12.0	4.0
1-phenyl-1-propanol	0.3	0.7	0.4	0.7	2.7	14.0*	20.0*
9-fluorenone	0	3.0	43.0*	7.7	24.0	67.0*	83.4*
9,10- <i>H</i> -dihydroanthracene	0	0.7	5.0	0.7	0	16.4	5.0
fluorene	0	0	0	0	0	0	0

clear ones. In fact **2** is more active than **1** for all alcohols apart from 1-phenyl-1-propargyl alcohol. This is also the only case where **1** and **2** are slightly less active than **III** and **IV**, that is, the reactivity of this alcohol in combination with thiacalixarene-based catalysts has a special but unknown element. In contrast, the TOF for the oxidation of fluorenone catalyzed by **2** (83.4 h⁻¹) is twice as high as that observed for

III (43.0 h⁻¹) which in turn is almost twice as high as that of VO(acac)₂, and the TOF of **1** is remarkably high (67.0 h⁻¹), too, while the two mononuclear calixarene complexes **I** and **II** show almost no activity. Having found that thiacalixarene complexes **1** and **2** are more active catalysts for alcohol oxidation than classical calixarene complexes **I–IV**, we tested whether they can also catalyze the oxidation of activated C–H bonds in unfunctionalized hydrocarbons such as 9,10-dihydroanthracene. Of all complexes investigated **1** performs best (16.4 h⁻¹), while **2** is as active as **III**. The oxidation products were identified for **1** (**2**) as 8.2% (0.3%) anthracene, 4.1% (2.3%) 10*H*-anthracene-9-one, and 4.1% (2.4%) 9,10-dihydroanthracene-9,10-diol. Formation of the ketone and the diol probably proceeds via anthranol by analogy with a corresponding Ru-catalyzed oxidation.^[17] However, with fluorenone as a substrate whose C–H bonds are somewhat (ca. 23 kJ mol⁻¹) stronger, none of the compounds showed any activity.

Active species and oxidation mechanism: First, experiments were carried to ensure that apart from removing the water generated in ODH, the molecular sieves do not play any other decisive role during catalysis: In the case of catalysts that are reasonably stable to water (e.g., **III**) the same results can be obtained in the absence of molecular sieves, too.

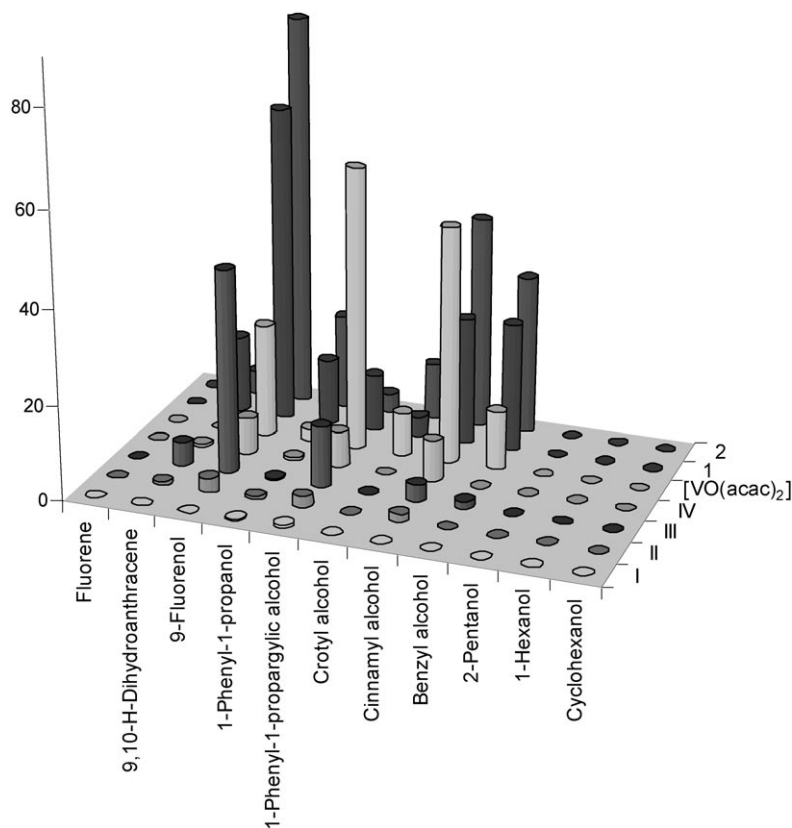


Figure 3. Three-dimensional plot of the data in Table 1. The numbers refer to TOFs [h⁻¹] calculated per vanadium center.

During the catalytic experiments involving **1** and **2** some interesting additional observations were made. When **1** was employed as a potential catalyst for the oxidation of inert substrates (1-hexanol, 2-pentanol, cyclohexanol, and 9-fluorenone), the workup procedure involving filtering through untreated (i.e., wet) filter pulp led to a change of color from brown to red, and from the resulting solution considerable amounts of red crystals of **2** could be precipitated. This was surprising, as hydrolysis of **1** gives free H₄TC (and not **2**), but it can be rationalized by assuming that **1** acts as precatalyst being converted to the active catalyst under catalytic conditions (by warming to 80 °C or reaction with O₂), which in contact with water is hydrolyzed to give **2** (**2** escapes further hydrolysis to give H₄TC by precipitation). We found that heating a solution of **1** to 80 °C in the presence of molecular sieves but in the absence of alcohol and O₂ leads to a color

change from purple (**1**) to brown, and this solution provides red **2** on contact with water. The intermediate brown product was isolated and purified by crystallization from dichloromethane. Analysis of the crystals by IR and ^1H NMR spectroscopy, mass spectrometry, and single-crystal X-ray diffraction showed that they belonged to the thia analogue of **1**: $\text{PPh}_4[(\text{TC})\text{V}=\text{O}]$ (**3**), which was formed from **1** by double intramolecular HCl elimination initiated by heating. Unlike the anion of **1**, that of **3** adopts the partial cone structure (paco) in the crystal (Figure 4, Scheme 3).

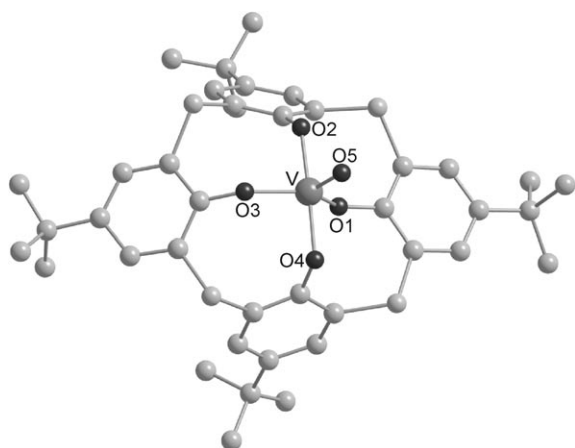
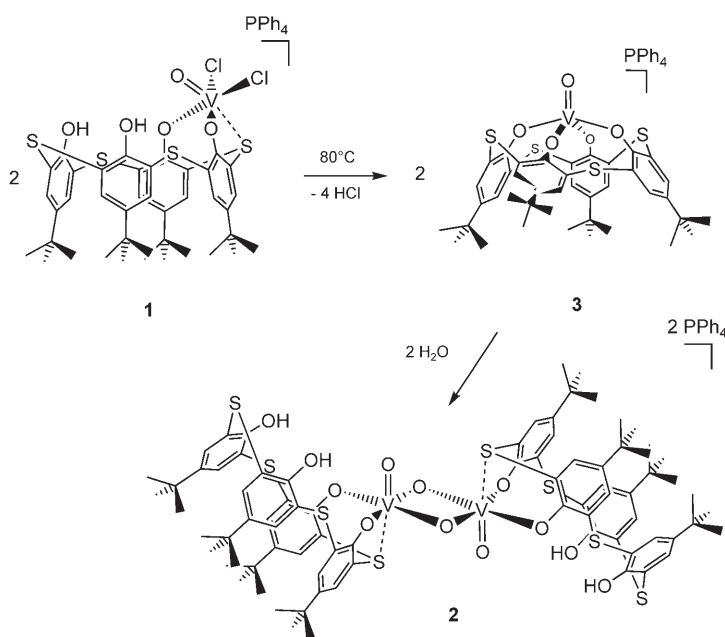


Figure 4. Molecular structure of the anion of **3**. All hydrogen atoms, the Ph_4P^+ ions, and cocrystallized CH_2Cl_2 and hexane solvent molecules omitted for clarity. There are two anions and two cations in the asymmetric unit of the unit cell; the following data are presented for one of these anions. Selected bond lengths [Å] and angles [°]: O1–V 1.556(7), O2–V 1.861(8), O3–V 1.947(8), O4–V 1.863(7), O5–V 1.916(8); O1–V–O2 119.4(4), O1–V–O3 94.2(4), O1–V–O4 108.0(4), O1–V–O5 93.9(4), O2–V–O4 132.6(3), O3–V–O5 171.5(3), V–(O1, O2, O4) 0.013(2).



Scheme 3.

While the vanadium atom in **1** has a square-pyramidal coordination sphere, due to the paco conformation, that in **3** is coordinated in a trigonal bipyramidal fashion with O3 and O5 as axial ligands (O3–V–O5 171.5(3)°). The vanadium atom is located almost exactly within the trigonal plane defined by O1, O2, and O4: the distance of V from that plane is only 0.013(2) Å. The V–O1 bond length of 1.556(7) Å is in the normal range observed for V=O units in calixarene ligand environments, and in the absence of S coordination, the V–OAr bonds have typical lengths, too.

The ^1H NMR spectrum of **3** in CD_3CN corresponds to a C_4 -symmetric molecule: only one singlet is observed for all aryl protons, and the protons of the *tert*-butyl groups give rise to only one signal, too. Thus, in solution the thiacalixarene ligand of **3** is either highly dynamic, so that an averaged symmetric structure is shown by the ^1H NMR spectrum (however, lowering the temperature to -50°C did not alter the spectrum), or it simply switches from the paco to the cone structure. Radius et al.^[18] showed by X-ray crystallography and NMR investigations that calix[4]arene complexes of d^0 metals (e.g., Mo and Ti) can undergo cone/paco isomerization. Apparently, in case of the d^0 V=O complex **3** the two conformations are very close in energy (we found evidence for such a situation earlier^[8]) and the environment determines which conformation is adopted.

Identification of **3** provides much valuable information. First, it shows that whenever **1** is employed as catalyst at 80°C , **3** will be generated in situ as active species. Reaction of **3** with convertible alcohols is indicated by a further color change, and most likely this yields the carbonyl compounds. O_2 is then needed to reoxidize the V center, and apparently this leads back to **3** again. Second, it is also clear that hydrolysis reactions do not play any role during the catalytic processes, as **1** and **2** give different catalytic results; that is, the molecular sieves remove the water generated during alcohol oxidation very efficiently.

So far we were not able to identify any of the intermediates in the catalytic cycle involving **3** in contact with alcohols. However, we were more successful in the case of **2**: Treating **2** with two equivalents of fluorenol, whose oxidation is efficiently catalyzed by **2**, at 80°C in the absence of O_2 led to a color change from red to light green, and layering a CH_2Cl_2 solution of the reaction products with hexane led to chartreuse crystals.

Characterization by X-ray crystallography, elemental analysis, magnetic measurements, and IR spectroscopy identified the corresponding compound as $(\text{PPh}_4)_2[\{(\text{H}_2\text{TC})\text{V}\}_2(\mu\text{-OH})(\mu\text{-OC}_{13}\text{H}_9)]$ (**4**). The molecular structure of its dianion is shown in Figure 5. It is very similar to that of **2**, as it can be derived by formally replacing one of the $\mu\text{-O}$ bridges in **2** by a $\mu\text{-OH}$ ligand (the proton could be located in the X-ray analysis) and the other by a fluorenolate ligand (distinguished from a potential neutral fluorenone ligand by the angles around C81). Naturally, the exchange of the divalent oxo ligands by monovalent bridges is accompanied by a lengthening of the V–O bonds within this core (O6–V1 1.981(4) Å, O7–V1 1.992(4) Å, O6–V2 1.993(4) Å, O7–V2

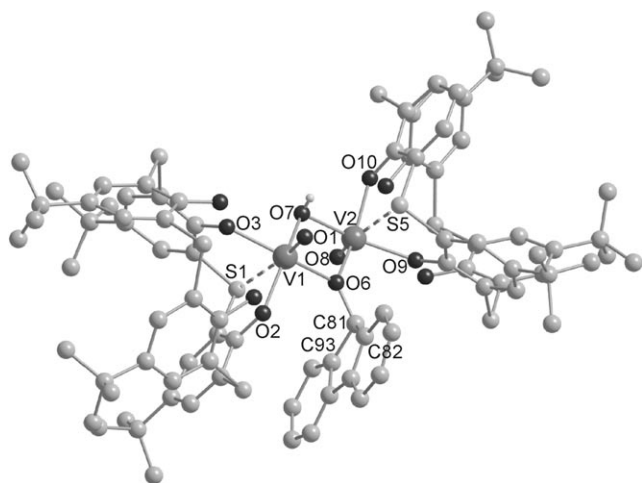
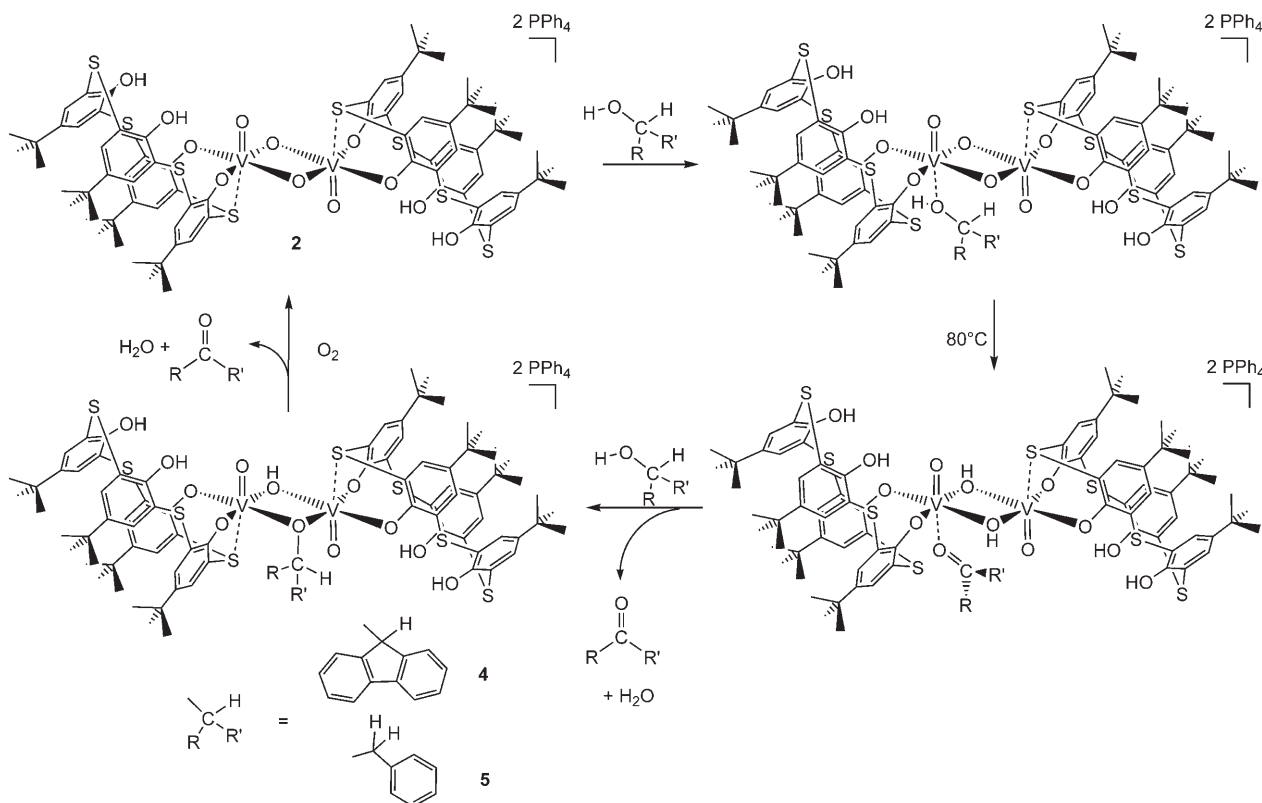


Figure 5. Molecular structure of the dianion of **4**. All hydrogen atoms, the Ph_4P^+ ions, and cocrystallized CH_2Cl_2 solvent molecules omitted for clarity. Selected bond lengths [\AA] and angles [$^\circ$]: O1–V1 1.595(5), O2–V1 1.992(4), O3–V1 2.035(5), O6–V1 1.981(4), O7–V1 1.992(4), S1–V1 2.771(2), O6–V2 1.993(4), O7–V2 1.971(4), O8–V2 1.598(5), O9–V2 2.035(5), O10–V2 2.002(4), S5–V2 2.795(3), V1–V2 3.1275(16); V1–O6–V2 103.81(17), V1–O7–V2 104.25(17), V1–O6–C81 129.4(3), V2–O6–C81 126.7(3), O6–C81–C82 116.2(5), O6–C81–C93 117.2(5), V1–O4 0.361(1), V2–O4 0.376(1), O7–H 0.834(18), V1–O7–H 109(2), V2–O7–H 110(2), O6–V1–O7–H 119.6(17), O6–V2–O7–H 118.5(17), Ar(O6)–Ar(O2) 13.3(3) $^\circ$.

1.971(4) \AA). A further consequence is that both vanadium atoms are now in the oxidation state +IV, that is, in a d^1 configuration that in principle could lead to a V–V bond.

However, probably due to the quite large V...V distance of 3.1275(16) \AA (**2**: 2.7453(6) \AA), such a bond is not formed, as indicated by the paramagnetism of **4**. As in comparable complexes^[13a,19] the two d^1 centers exhibit weak antiferromagnetic coupling already at room temperature ($\mu_{\text{eff}} = 1.97 \mu_{\text{B}}$). How is **4** formed? Scheme 4 shows a possible catalytic cycle involving **4**. It is not clear whether prebinding of the alcohol is necessary for the oxidation step, but if this were the case, it most likely occurs at one of the V centers by replacement of the weakly bound, soft thioether donor of the calixarene ligand, as shown in Scheme 4. The next steps could consist of dehydrogenation (possibly in the form of two consecutive H-atom abstractions) leading to fluorenone and a complex with two hydroxide bridges. In the presence of O_2 this could in principle be oxidized back directly to give **2** with elimination of water (this would, however, require only two of the four oxidation equivalents of O_2). In the absence of O_2 replacement of one of the two hydroxide bridges by an alcoholate ligand occurs to give **4**, and we prefer this mechanistic version also for the situation when O_2 is present considering the excess of alcohol in solution under catalytic conditions. O_2 could then oxidize **4** to give a second equivalent of fluorenone and the starting material **2**; this process involves four electrons and two protons, which in combination with O_2 lead to one equivalent of water and the O^{2-} ligand necessary to regenerate **2**. This mechanistic proposal is supported by the following additional observations:



Scheme 4.

- 1) According to Scheme 4 the reaction of **2** with two equivalents of fluorenol in the absence of O₂ should lead not only to **4** but also to one equivalent of fluorenone, which was indeed identified in the expected amount after workup of the mother liquor separated from **4**.
- 2) Reaction with only one equivalent of fluorenol again leads to **4** and unconverted **2**.
- 3) The reaction of **4** with O₂ readily leads to **2** and fluorenone, even at room temperature

Hence, this catalytic cycle for the oxidation of fluorenol with O₂ mediated by **2** is plausible, and it also seems to be applicable to oxidation of other alcohols: after analogous treatment of **2** with benzyl alcohol a corresponding derivative of **4**, namely, **5** (Scheme 4), was isolated, and it shows a very similar crystal structure. Thus, there seems to be a general mechanism for alcohol oxidations catalyzed by **2**, and several arguments hint at a cycle as displayed in Scheme 4. Interestingly, oxidation chemistry preferably takes place at the bridging oxo ligands and not at the terminal oxo ligands. This in turn means that the conclusion drawn for the function of **2** can not be valid for the other calixarene-based catalysts (**I–IV** and **1/3**), since each of those has its individual features and none of them contains a bis(μ -oxo) unit. However, the mechanism in Scheme 4 exemplifies why it may be advantageous for a catalyst to contain two V centers: all oxidation equivalents of O₂ are consumed within one cycle and the vanadium centers only have to switch oxidation states between +V and +IV, while the functioning of mononuclear catalysts requires a change between +V and +III. This raises the question whether the cooperation of two metal centers is in fact a prerequisite for this catalysis, in which case mononuclear catalyst **3** would have to operate by a mechanism involving two catalyst molecules, and this could explain the lower TOFs, too. However, that does not seem to be the case: preliminary kinetic investigations did not indicate any influence of catalyst concentration on the rate constants beyond that expected for a mechanism based on just one independent active site (probably involving V^{III}), that is, bimetallic catalysis is only open to dinuclear complex **2**, and this apparently renders it intrinsically superior for the reasons outlined above. This finding could in principal apply to the ODH of alcohols by surface sites, too, that is, dinuclear sites containing bridging oxo ligands should be more active than mononuclear ones. It will be interesting to follow up this working hypothesis in the future.

Conclusion

Syntheses and characterization of a mononuclear (**1**) and a dinuclear (**2**) oxovanadium thiacalixarene complex has been achieved. Both proved to be efficient catalysts for the oxidation of activated alcohols with O₂ and are superior to corresponding oxovanadium complexes with classical calixarene ligands. Complex **1** acts only as precatalyst that is converted to the active complex **3** on raising the temperature. Dinu-

clear complex **2** was often significantly more active than **1**. Both complexes were also capable of oxidizing an unfunctionalized hydrocarbon like 9,10-dihydroanthracene, although the TOFs are lower in comparison to those found for alcohol oxidation. Mechanistic studies on **2** led to isolation of an intermediate of the catalytic cycle involving **2**/O₂/fluorenol. Its formation and other mechanistic findings hint at cooperative behavior of the two vanadium centers that facilitates alcohol oxidation and reoxidation of the reduced catalyst. Moreover, dehydrogenation takes place preferably at μ -oxo ligands if these are present beside terminal oxo ligands. These findings are valuable for structure–function discussions in homogeneous oxidation catalysis and they may even have implications for mechanistic debates concerning active sites in ODH of alcohols on heterogeneous vanadia catalysts.

With regard to the mechanism suggested for catalyst **2** it seems interesting to investigate what kind of reactivity forms the basis for the activity of mononuclear complexes. A further mechanistic question that remains unanswered is the reason for the better performance of the thiacalixarene complexes in comparison to **I–IV**. A striking result is the high activity observed for **3**, which is identical with that of **1**, while the calixarene analogue **I** is inert. The rate-determining step (probably alcohol conversion) seems to be electronically accelerated by the thioether functions. More detailed and extensive studies may provide some insight in future.

Experimental Section

General procedures: All manipulations were carried out in a glove box or by Schlenk-type techniques with a dry argon atmosphere. The ¹H, ¹³C, and ⁵¹V NMR spectra were recorded on a Bruker AV 400 NMR spectrometer (¹H 400.13 MHz, ¹³C 100.63 MHz, ⁵¹V 105.25 MHz) with CH₂Cl₂, CD₃CN, or [D₆]DMSO as solvent at 20 °C. The ¹H NMR spectra were calibrated against the residual proton and natural-abundance ¹³C resonances of the deuterated solvent (CH₂Cl₂: $\delta_{\text{H}}=5.32$, CD₃CN: $\delta_{\text{H}}=1.93$, and [D₆]DMSO: $\delta_{\text{H}}=2.50$ ppm), and the ⁵¹V NMR spectra against VOCl₃ as standard. Microanalyses were performed on a Leco CHNS-932 elemental analyzer. Infrared spectra were recorded on samples prepared as KBr pellets with a Digilab Excalibur FTS 4000 FTIR-spectrometer. Magnetic moments μ_{eff} were measured on an Alfa Magway MSB Mk1 magnetic balance at room temperature. For this purpose the pure substance was levigated in an agate mortar, transferred into a glass capillary, and compressed. The recorded data were adjusted by using data from diamagnetic starting material as the background.

Materials: Solvents and Et₃N were purified, dried, and degassed prior to use. Pure Ph₄P[VO₂Cl₂]^[20] and *p*-tert-butylthiacalix[4]arene^[10a] were prepared according to the literature procedures. Alcohols were used as delivered without purification.

PPh₄[(H₂TC)VOCl₂] (1): H₂TC (0.25 g, 0.35 mmol) was dissolved in THF (40 mL) and treated with Ph₄P[VO₂Cl₂] (0.17 g, 0.35 mmol) dissolved in THF (20 mL). The resulting solution was stirred at room temperature, and the color changed from bright green to dark purple within a few minutes. After stirring for 4 h the solvent was removed in vacuo and the residual dark solid extracted with CH₂Cl₂ (15 mL). Addition of hexane (40 mL) led to a precipitate that was isolated by filtration and subsequently dissolved in CH₂Cl₂ (10 mL). The resulting solution was overlaid with hexane (40 mL) and stored at 5 °C. Over one day, **1**·CH₂Cl₂ (0.38 g, 85 %) precipitated as a dark purple solid, which was dried in vacuo. Elemental analysis calcd (%) for C₆₄H₆₆Cl₂O₃PS₄V·CH₂Cl₂: C

60.93, H 5.35, S 10.01; found: C 60.50, H 5.38, S 9.18; ¹H NMR (400 MHz, CD₂Cl₂, 25 °C): δ = 9.51 (s, 2H; ArOH), 7.92 (m, 4H; Ph₄P⁺), 7.78 (m, 8H; Ph₄P⁺), 7.65 (m, 8H; Ph₄P⁺), 7.61 (d, ⁴J(H,H) = 2.5 Hz, 2H; ArH), 7.58 (d, ⁴J(H,H) = 2.5 Hz, 2H; ArH), 7.53 (d, ⁴J(H,H) = 2.5 Hz, 2H; ArH), 7.46 (d, ⁴J(H,H) = 2.5 Hz, 2H; ArH), 1.18 ppm (2s, 36H; C(CH₃)₃); ¹³C NMR (100 MHz, CD₂Cl₂, 25 °C): δ = 169.2 (s; ArS), 168.9 (s; ArS), 156.7 (s; ArS), * 147.1 (s; ArrBu), 143.2 (s; ArrBu), 136.6 (s; ArH), 135.9 (brs; ArH), 135.8 (d, J(C,P) = 2.9 Hz, Ph₄P⁺), 134.5 (d, J(C,P) = 10.3 Hz; Ph₄P⁺), 133.5 (s; ArH), 130.7 (d, J(C,P) = 12.9 Hz; Ph₄P⁺), 133.1 (s; ArH), 124.8 (s; ArO), 121.1 (s; ArOH), 117.5 (d, J(C,P) = 89.6 Hz; Ph₄P⁺), 34.2 (s; C(CH₃)₃), * 31.04 (s; C(CH₃)₃), 30.9 ppm (s; C(CH₃)₃); * = according to HMBC measurements these signals cover the resonances of two different C atoms; ⁵¹V NMR (105 MHz, CD₂Cl₂, 25 °C): δ = -366 ppm (brs); IR (KBr): ν̄ = 3370 (m), 3057 (w), 2962 (s), 2904 (m), 2867 (m), 1475 (m), 1454 (m), 1440 (s), 1394 (w), 1364 (w), 1340 (vw), 1291 (m), 1275 (s), 1261 (s), 1245 (m), 1186 (w), 1107 (s), 995 (m), 981 (s), 968 (m), 958 (m), 890 (m), 838 (m), 749 (s), 723 (s), 689 (s), 621 (m), 550 (m), 527 (s), 469 (m), 447 (m), 432 (m) cm⁻¹.

(PPh₄)₂[{H₂TCV(O)(μ-O)}₂] (2): H₄TC (0.41 g, 0.56 mmol) was dissolved in CH₃CN (10 mL) and Et₃N (0.16 mL, 1.1 mmol) was added. Subsequently, 0.28 mg (0.56 mmol) of Ph₄P[VO₂Cl₂] dissolved in CH₃CN (10 mL) was added via cannula, and the color immediately changed to red and finally red-brown. Stirring for 30 min at room temperature yielded pure **2** as a red precipitate (0.51 g, 75%), which was collected. On cooling of the mother liquor a further fraction of **2** (35 mg, 5%) crystallized that had to be washed several times with small amounts of CH₃CN to remove contaminants. Elemental analysis calcd (%) for C₁₂₈H₁₃₂O₁₂P₂S₈V₂·3CH₃CN: C 66.89, H 5.91, N 1.75, S 10.65; found: C 66.67, H 6.22, N 1.72, S 10.95; ¹H NMR (400 MHz, [D₆]DMSO, 25 °C): δ = 10.90 (s, 2H; OH), 7.96 (m, 4H; Ph₄P⁺), 7.82 (m, 8H; Ph₄P⁺), 7.74 (m, 8H; Ph₄P⁺), 7.67 (d, ⁴J(H,H) = 2.5 Hz, 2H; ArH), 7.60 (d, ⁴J(H,H) = 2.5 Hz, 2H; ArH), 7.53 (d, ⁴J(H,H) = 2.5 Hz, 2H; ArH), 7.49 (d, ⁴J(H,H) = 2.5 Hz, 2H; ArH), 1.19 (s, 18H; C(CH₃)₃), 1.15 ppm (s, 18H; C(CH₃)₃); ¹³C NMR (100 MHz, [D₆]DMSO, 25 °C): δ = 166.8 (s; ArS), 158.7 (s; ArS), 142.3 (s; ArrBu), 140.8 (s; ArrBu), 136.4 (s, ArH), 135.6 (d; J(C,P) = 3.0 Hz; Ph₄P⁺), 135.4 (s; ArH), 135.2 (s; ArH), 135.0 (s; ArS), 134.8 (d, J(C,P) = 10.5 Hz; Ph₄P⁺), 134.13 (s; ArH), 130.6 (d, J(C,P) = 12.7 Hz; Ph₄P⁺), 130.5 (s; ArS), 124.1 (s; ArO), 123.5 (s; ArOH), 118.3 (s; CH₃CN), 116.5 (d, J(C,P) = 84.5 Hz; Ph₄P⁺), 34.1 (s; C(CH₃)₃), * 34.0 (s; CH₃CN), 31.6 (s; C(CH₃)₃), 31.5 ppm (s; C(CH₃)₃); * = according to HMBC measurements this signal covers the resonances of two different C atoms; ⁵¹V NMR (105 MHz, [D₆]DMSO, 25 °C): δ = -466 ppm (brs); IR (KBr): ν̄ = 3351 (w), 3056 (w), 2959 (s), 2903 (m), 2866 (m),

1587 (w), 1478 (s), 1458 (s), 1436 (s), 1392 (m), 1361 (m), 1305 (w), 1284 (w), 1257 (s), 1187 (w), 1109 (s), 997 (w), 962 (m), 885 (m), 838 (m), 752 (m), 723 (s), 686 (m), 657 (w), 618 (w), 525 (s), 425 (m) cm⁻¹.

PPh₄[(TC)V=O] (3): Compound **1** (0.30 g, 0.25 mmol) was dissolved in acetonitrile (10 mL) and molecular sieves (3 Å, 2 g) were added. The purple suspension was stirred at 80 °C for 2 h and the color changed to brown. After filtration all volatile substances were evaporated and the brown residue was taken up in CH₂Cl₂ (5 mL). The product precipitated after addition of hexane. Within a few days dark plates grew, which were collected (0.20 g, 71%). Elemental analysis calcd (%) for C₆₄H₆₄O₃PS₄V·0.25CH₃CN: C 68.34, H 5.76, N 0.31, S 11.31; found: C 68.47, H 6.31, N 0.19, S 10.73; ¹H NMR (400 MHz, CD₃CN, 25 °C): δ = 7.96 (m, 4H; Ph₄P⁺), 7.82 (m, 8H; Ph₄P⁺), 7.74 (m, 8H; Ph₄P⁺), 7.53 (s, 8H; ArH), 1.22 ppm (s, 36H; C(CH₃)₃); ¹³C NMR (100 MHz, CD₂Cl₂, 25 °C): δ = 167.6 (s; ArO), 143.5 (s; ArrBu), 135.5 (d, J(C,P) = 3.0 Hz; Ph₄P⁺), 134.6 (d, J(C,P) = 10.5 Hz; Ph₄P⁺), 132.3 (s; C_{ArH}), 130.5 (d, J(C,P) = 12.9 Hz; Ph₄P⁺), 123.0 (s; ArS), 117.6 (d, J(C,P) = 89.6 Hz; Ph₄P⁺), 33.9 (s; C(CH₃)₃), 31.6 ppm (s; C(CH₃)₃); ⁵¹V NMR (105 MHz, CD₂Cl₂, 25 °C): δ = -259 ppm (s); IR (KBr): ν̄ = 3058 (w), 2962 (s), 2904 (m), 2867 (m), 1587 (w), 1478 (m), 1465 (m), 1437 (s), 1421 (s), 1393 (m), 1361 (w), 1269 (s), 1260 (s), 1190 (w), 1108 (s), 997 (m), 906 (w), 886 (m), 836 (m), 766 (m), 753 (m), 723 (s), 689 (s), 559 (w), 527 (vs), 434 (w) cm⁻¹.

(PPh₄)₂[(H₂TCV)(μ-OH)(μ-OR)] (R = fluorenyl; **4; R = benzyl; **5**):** For the preparation of **4**, **2** (0.50 g, 0.22 mmol) was treated with two equivalents of fluorenyl (80 mg, 0.44 mmol) in acetonitrile solution (15 mL) at 80 °C for 2 h. The resulting light green solution was evaporated to dryness. After extraction with CH₂Cl₂ (4 mL) and layering of the resulting solution with *n*-hexane, chartreuse prisms (**4**·5CH₂Cl₂) and light teal needles (**4**·4CH₂Cl₂·C₆H₁₄) precipitated over a few days (0.24 g, 45%). Elemental analysis calcd (%) for C₁₄₁H₁₄₂O₁₂P₂S₈V₂·0.75CH₂Cl₂: C 67.76, H 5.76, S 10.21; found: C 67.77, H 6.15, S 9.80; μ_{eff} = 1.97 μ_B; IR (KBr): ν̄ = 3671 (w), 3060 (w), 2961 (m), 2902 (m), 2867 (m), 1587 (w), 1480 (vs), 1443 (vs), 1393 (m), 1361 (m), 1310 (m), 1256 (s), 1192 (m), 1108 (s), 1050 (m), 982 (m), 883 (m), 839 (s), 792 (w), 752 (vs), 739 (vs), 723 (vs), 689 (s), 670 (m), 628 (w), 529 (s), 428 (m) cm⁻¹.

Compound **5** can be prepared analogously; it can be isolated in the form of light green needles, which were characterized by single crystal X-ray analysis and IR spectroscopy (see Supporting Information).

Oxidation studies: Catalyst (for **1** 0.01 mmol; for **2** only 0.005 mmol due to the dinuclear nature of the complex, which in principle could lead to twofold activity in comparison with **1** in the absence of any additional effects) was dissolved in acetonitrile (1.5 mL). After addition of molecular

Table 2. Crystal data and structure refinement of **1–4**.

	1	2	3	4
formula	C ₆₄ H ₆₆ Cl ₂ O ₅ PS ₄ V·CH ₂ Cl ₂	C ₁₂₈ H ₁₃₂ O ₁₂ P ₂ S ₈ V ₂ ·2DMF	2C ₆₄ H ₆₄ O ₃ PS ₄ V·2CH ₂ Cl ₂ ·C ₆ H ₁₄	C ₁₄₁ H ₁₄₂ O ₁₂ P ₂ S ₈ V ₂ ·5CH ₂ Cl ₂
formula weight [g mol ⁻¹]	1281.22	2428.82	2502.62	2873.48
<i>T</i> [K]	180(2)	100(2)	100(2)	100(2)
<i>λ</i> [Å]	0.71073	0.79990	0.71073	0.71073
crystal system	monoclinic	triclinic	monoclinic	triclinic
space group	<i>P</i> 2 ₁ / <i>c</i>	<i>P</i> 1̄	<i>P</i> 2 ₁ / <i>c</i>	<i>P</i> 1̄
<i>a</i> [Å]	25.060(4)	13.715(3)	22.8776(14)	14.935(2)
<i>b</i> [Å]	11.7022(11)	21.149(4)	21.7059(9)	17.761(2)
<i>c</i> [Å]	24.096(4)	24.419(5)	25.9245(15)	27.557(4)
<i>α</i> [°]	90	66.22(3)	90	94.494(12)
<i>β</i> [°]	113.883(17)	83.90(3)	91.810(5)	103.370(11)
<i>γ</i> [°]	90	74.16(3)	90	97.056(11)
<i>V</i> [Å ³]	6461.3(16)	6236(2)	12867.1(12)	7014.5(17)
<i>Z</i>	4	2	4	2
<i>ρ</i> [g cm ⁻³]	1.230	1.294	1.292	1.360
μ(MoK _α) [mm ⁻¹]	0.435	0.573	0.440	0.525
<i>F</i> (000)	2504	2560	5256	2996
GoF	0.778	1.031	1.183	1.007
<i>R</i> ₁ [<i>I</i> > 2σ(<i>I</i>)]	0.0608	0.0357	0.1289	0.1269
<i>wR</i> ₂ (all data)	0.1456	0.0959	0.2746	0.2414
Δρ _{min} /Δρ _{max} [e Å ⁻³]	-0.655/0.741	-0.552/0.546	-0.691/0.953	-0.506/0.756

sieve powder (3 Å, 500 mg) alcohol (1.00 mmol) in acetonitrile (0.5 mL) was added. Subsequently, the mixture was stirred vigorously for 3 h (or for 1 h when 3 h led to a complete conversion) at 80 °C under a dioxygen atmosphere (oxygen was allowed to pass through the reaction vessel for 15 s before the reaction, and every 60 min this procedure was repeated). The mixture was then cooled to room temperature and the molecular sieve powder was separated by filtration through glass wool. In the case of alcohols (and resulting carbonyl compounds) with high boiling points, the acetonitrile solvent was then simply evaporated under vacuum. The conversion was determined by ¹H NMR spectroscopy. In the case of alcohols with low boiling points, the reaction mixture was filtered and directly employed in ¹H NMR spectroscopic investigations.

All starting materials and products are known and commercially available. The TOFs were calculated as the number of moles of substrate converted by 1 mol of catalyst per unit time.

Crystal structure determinations: Single crystals of **1** were obtained by overlaying a solution of **1** in CH₂Cl₂ with hexane at room temperature. Single crystals of **2** were obtained by cooling a solution of **2** in DMF to –30 °C. Single crystals of **3**, **4**, and **5** were obtained by layering a concentrated CH₂Cl₂ solution with *n*-hexane. The crystals were mounted on a glass fiber and then transferred into the cold nitrogen gas stream of the diffractometer (Stoe IPDS (**1**) and Stoe IPDS2T (**3**, **4**, **5**) using MoK_α radiation, λ = 0.71073 Å). The diffraction experiment for **2** was performed at Protein Structure Factory beamline 14.2 of BESSY and Free University Berlin at BESSY using synchrotron radiation (λ = 0.79990 Å). All structures were solved by direct methods (SHELXS-97)^[21] and refined versus F² (SHELXL-97)^[22] with anisotropic temperature factors for all non-hydrogen atoms (Table 2). All hydrogen atoms were added geometrically and refined by using a riding model.

CCDC-638466 (**1**), CCDC-638467 (**2**), CCDC-638468 (**3**), CCDC-638469 (**4**), and CCDC-638470 (**5**) contain the supplementary crystallographic data for this paper. These data can be obtained free of charge from the Cambridge Crystallographic Data Centre via www.ccdc.cam.ac.uk/data_request/cif.

Spectroscopic data for **5** and plots of all crystal structures showing 30% ellipsoids are available as Supporting Information.

Acknowledgements

We are grateful to the Deutsche Forschungsgemeinschaft, the SFB 546, the Fonds der Chemischen Industrie, the BMBF and the Dr. Otto Röhm Gedächtnisstiftung for financial support. We thank C. Jankowski for the preparation of starting materials and acknowledge support by U. Mueller at BESSY for the diffraction experiment involving **2**.

- [1] D. A. Ruddy, N. L. Ohler, A. T. Bell, T. D. Tilley, *J. Catal.* **2006**, *238*, 277.
- [2] a) P. Marturano, L. Drozdova, A. Kogelbauer, R. Prins, *J. Catal.* **2000**, *192*, 236; b) L. J. Lobree, I. C. Hwang, J. A. Reimer, A. T. Bell, *Catal. Lett.* **1999**, *63*, 233; c) R. Joyner, M. Stockenhuber, *J. Phys. Chem. B* **1999**, *103*, 5963; d) M. G. Clerici, P. Ingallina, *J. Catal.* **1993**, *140*, 71.
- [3] a) A. Comite, A. Sorrentino, G. Capannelli, M. Di Serio, R. Tesser, E. Santacesaria, *J. Mol. Catal. A* **2003**, *198*, 151; b) R. Zhou, Y. Cao, S. Yan, J. Deng, Y. Liao, B. Hong, *Catal. Lett.* **2001**, *75*, 107; c) T. Blasco, A. Galli, J. M. Lopez Nieto, F. Trifido, *J. Catal.* **1997**, *169*, 203; d) M. A. Chaar, D. Patel, H. H. Kung, *J. Catal.* **1988**, *109*, 463; e) A. Corma, J. M. Lopez Nieto, N. Paredes, *J. Catal.* **1993**, *144*, 425; f) F. D. Hardcastle, I. E. Wachs, *J. Mol. Catal.* **1988**, *46*, 173; g) G. Deo, I. E. Wachs, J. Haber, *Crit. Rev. Surf. Chem.* **1994**, *4*, 141; h) I. E. Wachs, B. M. Weckhuysen, *Appl. Catal. A* **1997**, *157*, 67; i) J. G. Eon, R. Olier, J. C. Volta, *J. Catal.* **1994**, *145*, 318; j) T. Balsko, J. M. Lopez Nieto, *Appl. Catal. A* **1997**, *157*, 117; k) A. Khodakov, B. Olthof, A. T. Bell, E. Iglesia, *J. Catal.* **1999**, *181*, 205; l) A. Khodakov, J. Yang, S. Su, E. Iglesia, A. T. Bell, *J. Catal.* **1998**, *177*, 343; m) E. V. Kondratenko, M. Baerns, *Appl. Catal. A* **2001**, *222*, 133; n) M. D. Argyle, K. D. Chen, E. Iglesia, A. T. Bell, *J. Catal.* **2002**, *208*, 139; o) L. Owens, H. H. Kung, *J. Catal.* **1993**, *144*, 202; p) O. R. Evans, A. T. Bell, T. D. Tilley, *J. Catal.* **2004**, *226*, 292.
- [4] a) S. Feyel, D. Schröder, H. Schwarz, *J. Phys. Chem. A* **2006**, *110*, 2647; b) S. Feyel, D. Schröder, H. Schwarz, *J. Phys. Chem. A* **2006**, *110*, 2647; c) S. Feyel, D. Schröder, X. Rozanska, J. Sauer, H. Schwarz, *Angew. Chem.* **2006**, *118*, 4793; *Angew. Chem. Int. Ed.* **2006**, *45*, 4677; d) S. Feyel, J. Döbler, D. Schröder, J. Sauer, H. Schwarz, *Angew. Chem.* **2006**, *118*, 4797; *Angew. Chem. Int. Ed.* **2006**, *45*, 4681; e) M. Engeser, D. Schröder, H. Schwarz, *Chem. Eur. J.* **2005**, *11*, 5975; f) X. Li, K. Nagaoka, L. J. Simon, R. Olindo, J. A. Lercher, A. Hofmann, J. Sauer, *J. Am. Chem. Soc.* **2005**, *127*, 16159; g) J. Döbler, M. Pritsche, J. Sauer, *J. Am. Chem. Soc.*, **2005**, *127*, 10861; h) M. Engeser, M. Schlangen, D. Schröder, H. Schwarz, T. Yumura, K. Yoshizawa, *Organometallics* **2003**, *22*, 3933; i) H. Fu, Z.-P. Liu, Z.-H. Li, W.-N. Wang, K.-N. Fan, *J. Am. Chem. Soc.* **2006**, *128*, 11114.
- [5] a) C. Limberg, *Angew. Chem.* **2003**, *115*, 6112; *Angew. Chem. Int. Ed.* **2003**, *42*, 5932; b) T. A. Hanna, *Coord. Chem. Rev.* **2004**, *248*, 429; c) C. Copéret, M. Chabanas, R. Petroff Saint-Arroman, J.-M. Basset, *Angew. Chem.* **2003**, *115*, 164.
- [6] a) V. Lorenz, F. T. Edelmann, *Z. Anorg. Allg. Chem.* **2004**, *630*, 1147; F. J. Feher, T. A. Budzichowski, *Polyhedron* **1995**, *14*, 3239; b) R. Duchateau, *Chem. Rev.* **2002**, *102*, 3525.
- [7] a) U. Radius, *Z. Anorg. Allg. Chem.* **2004**, *630*, 957; b) C. Floriani, *Chem. Eur. J.* **1999**, *5*, 19; c) C. Floriani, R. Floriani-Moro, *Adv. Organomet. Chem.* **2001**, *47*, 167; d) D. Buccella, G. Parkin, *J. Am. Chem. Soc.* **2006**, *128*, 16358.
- [8] E. Hoppe, C. Limberg, B. Ziemer, C. Mügge, *J. Mol. Catal. A* **2006**, *251*, 34.
- [9] E. Hoppe, C. Limberg, B. Ziemer, *Inorg. Chem.* **2006**, *45*, 8308.
- [10] a) H. Kumagai, M. Hasegawa, S. Miyanari, Y. Sugawa, Y. Sato, T. Hori, S. Ueda, H. Kamiyama, S. Miyano, *Tetrahedron Lett.* **1997**, *38*, 3971; b) N. Morohashi, F. Narumi, N. Iki, T. Hattori, S. Miyano, *Chem. Rev.* **2006**, *106*, 5291; c) J. Zeller, U. Radius, *Inorg. Chem.* **2006**, *45*, 9487; d) N. Iki, C. Kabuto, T. Fukushima, H. Kumagai, H. Takeya, S. Miyanari, T. Miyashi, S. Miyano, *Tetrahedron* **2000**, *56*, 1437; e) N. Iki, N. Morohashi, T. Suzuki, S. Ogawa, M. Aono, C. Kabuto, H. Kumagai, H. Takeya, S. Miyanari, S. Miyano, *Tetrahedron Lett.* **2000**, *41*, 2587; f) N. Morohashi, N. Iki, A. Sugawara, S. Miyano, *Tetrahedron* **2001**, *57*, 5557; g) N. Kon, N. Iki, S. Miyano, *Tetrahedron Lett.* **2002**, *43*, 2231; h) N. Kon, N. Iki, Y. Yamane, S. Shirasaki, S. Miyano, *Tetrahedron Lett.* **2004**, *45*, 207.
- [11] a) T. Kajiwara, S. Yokozawa, T. Ito, N. Iki, N. Morohashi, S. Miyano, *Chem. Lett.* **2001**, *6*; b) A. Bilyk, A. K. Hall, J. M. Harrowfield, M. W. Hosseini, G. Mislin, B. W. Skelton, C. Taylor, A. H. White, *Eur. J. Inorg. Chem.* **2000**, 823; c) T. Kajiwara, S. Yokozawa, T. Ito, N. Iki, N. Morohashi, S. Miyano, *Angew. Chem.* **2002**, *114*, 2180; *Angew. Chem. Int. Ed.* **2002**, *41*, 2076; d) K. Hirata, T. Suzuki, A. Noya, I. Takei, M. Hidai, *Chem. Commun.* **2005**, 3718; e) Z. Asfari, A. Bilyk, J. W. C. Dunlop, A. K. Hall, J. M. Harrowfield, M. W. Hosseini, B. W. Skelton, A. H. White, *Angew. Chem.* **2001**, *113*, 744; *Angew. Chem. Int. Ed.* **2001**, *40*, 721; f) A. Bilyk, A. K. Hall, J. M. Harrowfield, M. W. Hosseini, B. W. Skelton, A. H. White, *Aust. J. Chem.* **2000**, *53*, 895.
- [12] T. Sone, Y. Ohba, K. Moriya, H. Kumada, K. Ito, *Tetrahedron* **1997**, *53*, 10689, and references therein.
- [13] a) C. Redshaw, M. A. Rowan, L. Warford, D. M. Homden, A. Arbaoui, M. R. J. Elsegood, S. H. Dale, T. Yamato, C. P. Casas, S. Matsui, S. Matsuura, *Chem. Eur. J.* **2007**, *13*, 1090; b) B. Castellano, E. Solari, C. Floriani, R. Scopelliti, N. Re, *Inorg. Chem.*, **1999**, *38*, 3406; c) V. C. Gibson, C. Redshaw, M. R. J. Elsegood, *J. Chem. Soc. Dalton Trans.* **2001**, 767.
- [14] U. Heinzl, A. Henke, R. Mattes, *J. Chem. Soc. Dalton Trans.* **1997**, 501.
- [15] L. Liu, L. N. Zakharov, J. A. Golen, A. L. Rheingold, W. H. Watson, T. A. Hanna, *Inorg. Chem.* **2006**, *45*, 4247.

- [16] Y. Maeda, N. Kakiuchi, S. Matsumura, T. Nishimura, T. Kawamura, S. Uemura, *J. Org. Chem.* **2002**, *67*, 6718.
- [17] K. Kamata, J. Kasai, K. Yamaguchi, N. Mizuno, *Org. Lett.* **2004**, *6*, 3577.
- [18] U. Radius, *Inorg. Chem.* **2001**, *40*, 6637.
- [19] E. Garribba, G. Micera, E. Lodyga-Chruscinska, D. Sanna *Eur. J. Inorg. Chem.* **2006**, 2696.
- [20] a) P. Ehrlich, W. Engel, *Z. Anorg. Allg. Chem.* **1963**, *322*, 217; b) D. Fenske, A.-F. Shihada, H. Schwab, K. Dehnicke, *Z. Anorg. Allg. Chem.* **1980**, *471*, 140.
- [21] G. M. Sheldrick, SHELXS-97 Program for Crystal Structure Solution, University of Göttingen, **1997**.
- [22] G. M. Sheldrick, SHELXL-97 Program for Crystal Structure Refinement, University of Göttingen, **1997**.

Received: March 2, 2007

Published online: June 13, 2007